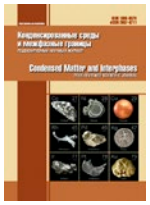

ISSN 1606-867X (Print)
ISSN 2687-0711 (Online)
Condensed Matter and Interphases
Kondensirovannye Sredy i Mezhfaznye Granitsy
https://journals.vsu.ru/kcmf/

Review

Review article
https://doi.org/10.17308/kcmf.2024.26/12396

Nonstoichiometry of refractory inorganic compounds with a volatile component determined by new methods of physicochemical analysis. Review

I. G. Vasilyeva

Nikolaev Institute of Inorganic Chemistry of Siberian Branch Russian Academy of Sciences
3 Lavrent'ev ave., Novosibirsk 630090, Russian Federation

Abstract

The nonstoichiometry of refractory compounds with a volatile component is based on solid-phase and heterophase processes. At the same time, measurements of the parameters of these high-temperature phase transformations are often inaccurate. The inaccuracy results from the instability of the equipment as well as the behavior of themselves samples. To overcome these limitations, we developed three new methods of physicochemical analysis, which were then used in a comprehensive approach to the study of nonstoichiometry and the chemical composition of defective phases at the macro and micro levels. We refer to are high-speed thermal analysis, static tensimetric membrane technique, and stoichiographic differential dissolution method. The methods were used to measure temperatures up to 2400 °C, pressure up to 10 atm, and the degree of nonstoichiometry up to 10^{-4} mol. %.

The review demonstrates the effectiveness of the proposed methodology applied to refractory compounds LnS, Ln_2S_3 (Ln = P3M), $Yb(Ln)_{14}MnSb_{11}$, $ZrGeO_4$, Zr_3GeO_8, MgO, and Mg(Ru)O, as well as highly volatile REM polychalcogenides and $ZnMo(W)O_4$, presented in the form of powders, large crystals, ceramics, and films. For each of the studied substances, fundamental knowledge was gained regarding their spatial-temporal evolution responsible for the occurrence and the degree of nonstoichiometry. The data was obtained by studying *T-x* and *p-T* diagrams and by using of the stoichiographic method to determine the phase purity, microstructural inclusions, and spatial chemical inhomogeneity of individual phases at a micro level.

The obtained new quantitative thermodynamic and physicochemical data regarding the nonstoichiometry of the studied compounds was used as a basis for the choice of the composition and the design of the crystallization process, sintering and chemical deposition of thin films to realize a directed synthesis of materials with the desired properties. The review was initiated by Professor Magomed Babanly, DSc in Chemistry, Associate Member of the Russian Academy of Sciences, and editor of the special issue of the journal *Condensed Matter and Interphases* dedicated to physicochemical analysis in material science.

Keywords: Refractory chemically unstable compounds, Physicochemical analysis, Phase diagrams, nonstoichiometry

Funding: The research was carried out with the financial support of the Ministry of Science and Higher Education of the Russian Federation under the Government Order by Nikolaev Institute of Inorganic Chemistry of the Siberian Branch of the Russian Academy of Sciences (agreement No. 21031700315-2).

For citation: Vasilyeva I. G. Nonstoichiometry of refractory inorganic compounds with a volatile component determined by new methods of physicochemical analysis. Review. *Condensed Matter and Interphases*. 2024;26(4): 633–645. https://doi.org/10.17308/kcmf.2024.26/12396

Для цитирования: Васильева И. Г. Нестехиометрия тугоплавких неорганических соединений с летучим компонентом через призму оригинальных методов физико-химического анализа. Обзор. *Конденсированные среды и межфазные границы*. 2024;26(4): 633–645. https://doi.org/10.17308/kcmf.2024.26/12396

✉ I. G. Vasilyeva, e-mail: kamars@niic.nsc.ru

1. Introduction

Nonstoichiometry plays a special role in inorganic material science since it solves practically important problem of controllability of the material characteristics. Current theoretical approaches to the nonstoichiometry of complex compounds do not allow an a priori prediction of its nature and scale in the temperature and pressure coordinates. Therefore, it is important to experimentally determine any dependences regarding the formation, structure, and properties of nonstoichiometric phases. Physicochemical analysis methods combined with a dynamic approach are predominantly used to study the equilibria that involve phases of variable composition. These methods help to discover new facts and dependences and play a crucial role in the development of new theories and synthesis of new compounds and materials with desired properties. Investigation of the nonstoichiometry of refractory chemically unstable compounds with active volatile components requires particular attention. Therefore, we developed a system of unique methods of thermal [1–2], tensimetric [3], and stoichiographic analysis [4–5], which helps to determine the key thermodynamic parameters of a system with the same accuracy and ensure the reliability of phase pictures.

Earlier we demonstrated a high effectiveness of these methods by providing a detailed characteristic of large single crystals of $AgGaS_2$, $AgGaGeS_4$, $ZnGeP_2$, and $LiMX_2$ (M = In, Ga; X = S, Se, Te) which contained volatile and chemically active components [6]. In that particular study we focused on the nonstoichiometry and the mechanisms of formation of intrinsic point and extended defects and their connection with optical properties. The degree of nonstoichiometry is presented by *T-x* and $p_{volatile}$-*T-x* diagrams, which served as a basis for the growth of the said crystals with an optical quality that would meet the requirements to materials used in nonlinear optics.

This review presents new data regarding high-temperature phase transformations of refractory sulfides and complex antimonides of rare earth metals (REM), as well as oxide compounds of systems Zn-Ge-O, Zn-Mo(W)-O, and $MgO-ZrO_2$, where even a small loss in volatile component significantly effects the structural state and functional properties. These compounds have different thermal stability and different scale of nonstoichiometry. Their phase transformations are susceptible to a large number of interferences including reactions with oxygen, which often distorts the results of the commonly used analysis methods. The review demonstrates that the use of effective methods and procedures specific for each system bring physicochemical experiments at a principally new level and develop a deeper understanding of the nature of nonstoichiometry of the studied compounds.

2. High-speed thermal analysis method (HSTA) [1–2]

The method is used in an atmosphere of a helium buffer at temperatures ranging from 500 to 2500 °C and pressures of up to 10 atm. It proved to be an innovative method both for studying the nonstoichiometry of REM antimonides and oxide compounds of Zn-Ge-O and Zn-Mo(W)-O, and for determining the conditions regulating the formation of their functional properties. Refractory sulfides of REM, LnS, and Ln_2S_3 are both promising high-temperature thermoelectrics and magnetic and optical materials. They are synthesized in the form of large crystals by means of melt crystallization and in the form of dense non-porous ceramics by means of electropulse sintering and dynamic hot pressing. The synthesis methods are based on p_s-*T-x* diagrams and the methodological variability of the HSTA approach, which helps to accurately determine the thermodynamic parameters (Fig. 1). The $p_{He} \gg p_S$ based methodology is used to reliably measure the liquidus and solidus temperatures and thus ensure the accuracy of the topology of the *T-x* diagram (Fig. 1a). The $p_{He} = p_S$ based methodology is used to measure the temperature at the boiling poin and to obtain an equilibrium *p-T* diagram of the dissociation process (Fig. 1b). The $p_{He} \ll p_S$ based methodology helps to obtain data regarding the nature and degree of nonstoichiometry, its initial and intermediate stages, and the kinetics of the transformations (Fig. 1c). The heating process is registered in several ways: automated recording of the heating curves d*U*/dτ (a derivative of the thermal emission along time), visual observation of the heated sample, and analytical data regarding the amount

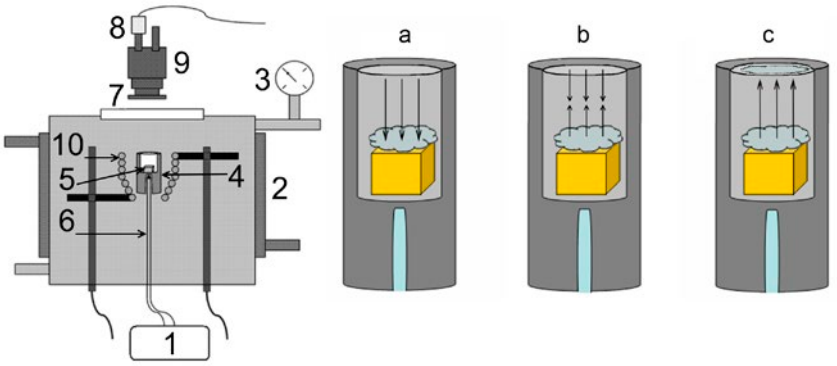

Fig. 1. Block synopsis setup and procedures used in the experiments. Setup: *1* – temperature control block, *2* – chamber; *3* – manometer, *4* – Mo holder, *5* – sample, *6* – thermocouple, *7* – quartz window, *8* – IR photodiode, *9* – microscope, *10* – tungsten heater. Procedures from the left to the right: (a) full preservation of composition, (b) equality of vapor pressures between sample and helium, (c) free evaporation with the vapor condensate formation

of the volatile component distributed between the condensate (on the sight glass of the crucible) and the solid residue. The crucible was calibrated with regard to the melting points of Au (1100 °C), Co (1493 °C), Pt (1772 °C), Rh (1963 °C), and Al_2O_3 (2050 °C) and the pressure of decomposition of GaAs crystals, with p = 1.0 atm at 1610 °C. The measurement accuracy of the melting points was 1 % and the measurement accuracy of the pressure was 5 %.

The experimental data regarding the La-S system is presented as p_S-T and T-x diagrams. The topology of the latter is also typical for the Nd-Sm systems (Fig. 2). The values T_{melt} = 2130 K and p_s = 2.3 atm are the operating parameters of the growth of large stoichiometric La_2S_3 crystals, and T_{press} = 1510 K and p_s = 0.016 atm resulted in the formation of stoichiometric ceramics of the La_2S_3, β and γ polymorphs with a good optical quality [7-9]. For HoS and GdS monosulfides, HSTA was effectively used to obtain the liquidus line in the temperature range of 2400–2700 K and sulfur compositions of 47–53 at. %, and to determine the homogeneity regions of both monosulfides, which had practically no oxygen dissolved in the sulfide matrix. The obtained data was used for the sintering process to obtain dense non-porous ceramics of monosulfides. HSTA was also used to detect small amounts of impurity oxide phases of REM. This helped us to synthesize oxygen-free ceramics when sintering powder mixtures Ho_2S_3+Ho and Gd_2S_3+GdH_2 using the electropulse technology [10–11].

Complex antimonides $A_{14-x}Me_xMnSb_{11}$, A = Yb, Eu, x = La-Lu (except for Eu and Ce) are known to be Zintl phases and promising high-

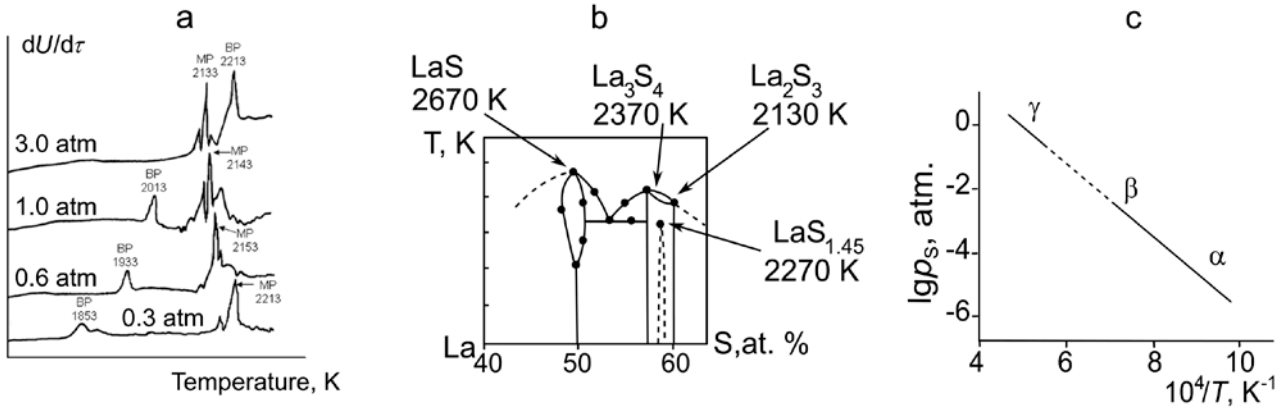

Fig. 2. Physicochemical study of the La–S system (a) heating curves of La_2S_3 with melting (MP) and boiling (BP) peaks in a function of the helium pressure; (b) top of T-x diagram of the condensed state of the La–S system; (c) p-T dependence for α, β and γ forms of La_2S_3

temperature thermoelectrics. The limitations of the physicochemical methods of analysis of these compounds were obvious due to the high melting points and the reactive nature of the melts. Reliable data regarding the phase state of the Eu-Mn-Sb system were obtained by HSTA and the *T-x* diagram of the Eu-Sb system with the data about the thermodynamic and thermochemical stability of binary antimonides presented in Fig. 3a. The thermodynamic data regarding the stable phases facilitated further synthesis of the desired ternary compound $Eu_{14}MnSb_{11}$ in the single-phase state by means of a direct reaction of Eu_4Sb_3 and $EuSb_2$ with manganese [12]. Diagrams of $Yb(Eu)Sb_2$-Mn and $Yb(Eu)_4Sb_3$-Mn were topologically identical with the Eu diagram tending to move towards higher temperatures. They were also used for the synthesis of single-phase ternary $Ln_{14}MnSb_{11}$ crystals according to the Ln_4Sb_3+Mn reaction and based on the similarity of the thermochemical parameters of phases Ln_4Sb_3 and Mn [13].

HSTA also contributed to the problem of enhancing the thermal stability of $Yb_{14}MnSb_{11}$ [14–15]. Long-term use of stoichiometric ceramics in aerospace vacuum at a temperature of 1000 °C is hindered by a high sublimation rate. By partially replacing ytterbium with other REM, the volatility of which was 5–10 orders of magnitude lower, well-shaped crystals were obtained from a $Yb_{14-x}Ln_xMn_6Sn_{86}$ solution melt with an excess of tin as a solvent. The limiting solubility of Ln cations, having various dimensions, was determined, as well as the specifics of their ordered distribution between three possible structural positions of Yb ions in the lattice of the ternary antimonide (Fig. 4a) [14]. This approach provided rising of the thermodynamic data (melting point) of 40 °C and lowering of thermochemical parameters (the mass loss) by 15 times of the doped samples, that are explained by the strengthening of the ionic bond in the lattice and lower mobility of the volatile ytterbium cation (Fig. 4b). With an idea to reduce the sublimation rate of $Yb_{14}MnSb_{11}$ by

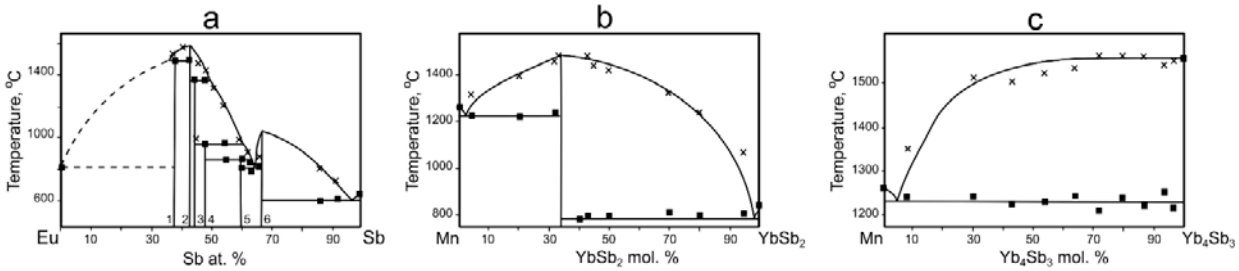

Fig. 3. a) *T-x* diagram of condensed state system Eu - Sb with the phases Eu_5Sb_3 – *1*, Eu_4Sb_3 – *2*, Eu_5Sb_4 – *3*, $Eu_{11}Sb_{10}$ – *4*, Eu_2Sb_3 – *5*, $EuSb_2$ – 6; (b) *T-x* diagram of the condensed state system Mn-$YbSb_2$; (c) *T-x* diagram of the condensed system Mn-Yb_4Sb_3

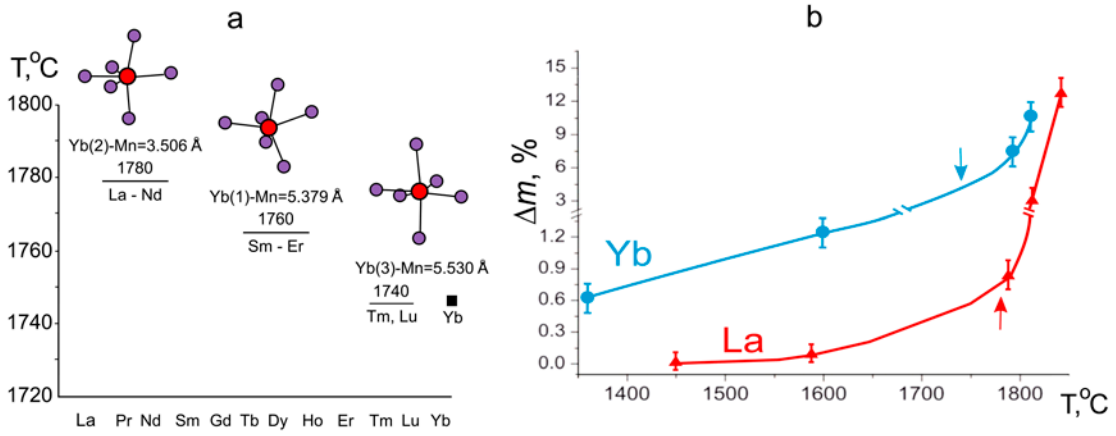

Fig. 4. Thermodynamic and thermochemical stabilities of the $Yb_{13.6}Ln_{0.4}MnSb_{11}$ phases: (a) T_{melt} as a function of the Ln distribution in the Yb (*1*), Yb (*2*), Yb (*3*) crystallographic positions; (b) mass loss of the $Yb_{14}MnSb_{11}$ (Yb), $Yb_{13.6}La_{0.4}MnSb_{11}$ (La) samples at temperatures before and after melting (marked by arrows)

creating a protective layer on the surface made of mixed Yb+Ln oxides, HSTA ensured reliable phase interpretation of complex products forming this layer [15]. This result was largely based on the analysis of the *T-x* diagrams of the system already been studied by us.

The nonstoichiometry of $ZnGeO_4$ and Zn_3GeO_8 is explained by an increased mobility of anionic lattice fragments responsible for the incongruent sublimation of these phases. To obtain reliable data regarding the thermochemical reactions and phase transformations of the samples heated to 2300 °C, all HSTA procedures were used: 1) quick and slow heating; 2) visual observation; 3) control of the distribution of the volatile GeO_2 between vapor and solid residue; 4) registration of the temperature of vapor condensation on the sight glass. New data regarding the nonstoichiometry of germanates was obtained, namely the existence of the initial small-scale stage of the GeO_2 loss resulting in the formation of subtraction solid solutions, and the final stage of the formation of the disordered ZrO_2 with 1–2 mol. % of GeO_2 (Fig. 5a). The suggested approach also proved the absence of the direct transition $ZrGeO_4 \rightarrow Zr_3GeO_8$ [16]. The findings regarding the nonstoichiometry and defectiveness of germanates contributed to the understanding of the mechanism of formation of active intermediate defects responsible for the sintering of initial powders (Fig. 5b), since this state is very important for formation of high-temperature non-porous ceramics.

The functional effectiveness of cryogenic scintillation detectors is ensured by a complete stoichiometry of large $ZnMo(W)O_4$ crystals obtained using the low-temperature-gradient Czochralski technique in a system semi-open to air. According to the *T-x* diagram of the $ZnO\text{-}MoO_3$ system, the $ZnMoO_4$ phase is linear. However, two negative factors, namely the peritectic melting of the phase and the incongruent evaporation of MoO_3, significantly affect the quality of the grown crystals. In [17], a number of highly precise measurements of the composition, density, and structural parameters were performed to determine the scale of nonstoichiometry of the grown $ZnMoO_4$ crystals with an excess of ZnO of 0.6 mol. %. The nonstoichiometry is described by oxygen vacancies and random distribution of zinc atoms among the possible molybdenum positions (antistructure disordering) and in interstitial sites. HSTA and the differential dissolution methods were used to determine the main sources of the MoO_3 loss. These methods allowed for precision diagnostics of the products during every stage of crystal growth in a semi-open in air system. The first stage of the solid-phase synthesis of the mixture of ZnO and MoO_3 powders at 650 °C demonstrated spatial inhomogeneity of seeds with the formation of a stable surface layer supersaturated with MoO_3 (Fig. 6a). The surface oxide sublimates actively during homogenization at 1010 °C and the crystallization occurs from a nonstoichiometric melt. Another source of the MoO_3 loss is the overheating of the melt resulting in dissociation of the molybdate anion to oxide and oxygen, which changes the composition of the melt (Fig. 6c). When WO_3 was added to a nonstoichiometric molybdate, the liquidus and solidus lines shifted significantly towards lower

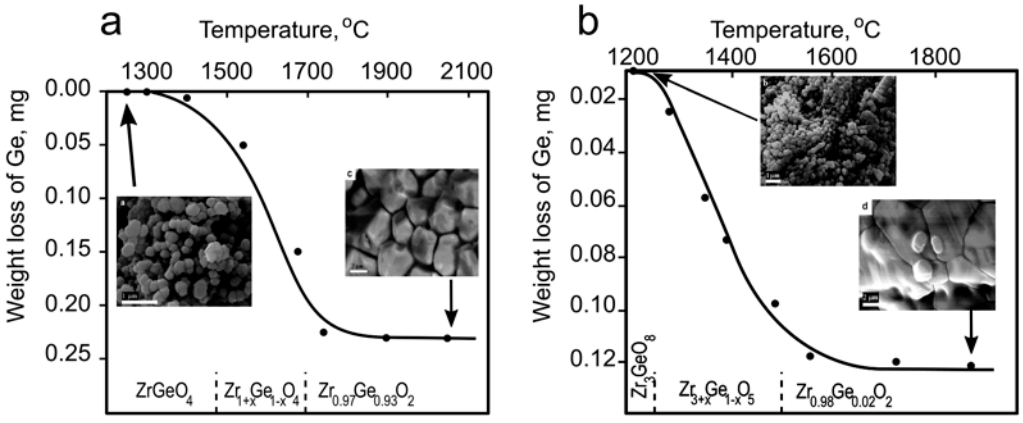

Fig. 5. High-temperature transformations of the $ZrGeO_4$ (a) and Zr_3GeO_8 (b) phases. Dependence of compositions from temperature (dashed lines); inserts - morphology of the initial and final samples

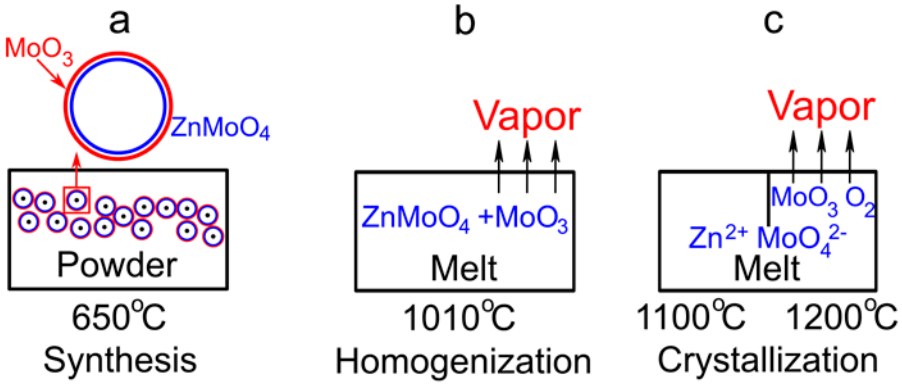

Fig. 6. Sources of formation and loss of the volatile MoO_3component of loss in a semi-open system: (a) during synthesis, (b) during homogenization, (c) during crystallization

temperatures. This kind of minimization of the negative effect of the peritectic melting enhances the quality of large $ZnMo(W)O_4$ crystals.

3. Static tensimetric membrane technique (STM) [3]

This method (Fig. 7a) used at temperatures of 300–1220 K and pressures of 0.01–2 atm thermodynamically determines the existence of nonstoichiometry by means of precise scanning of the composition of the initial sample in the temperature function (Fig. 7c) and can differentiate between several related compounds with very close, but various, compositions (Fig. 7 b). It is this method that played a key role in the understanding of the nature of the nonstoichiometry of REM dichalcogenides with volatile chalcogens.

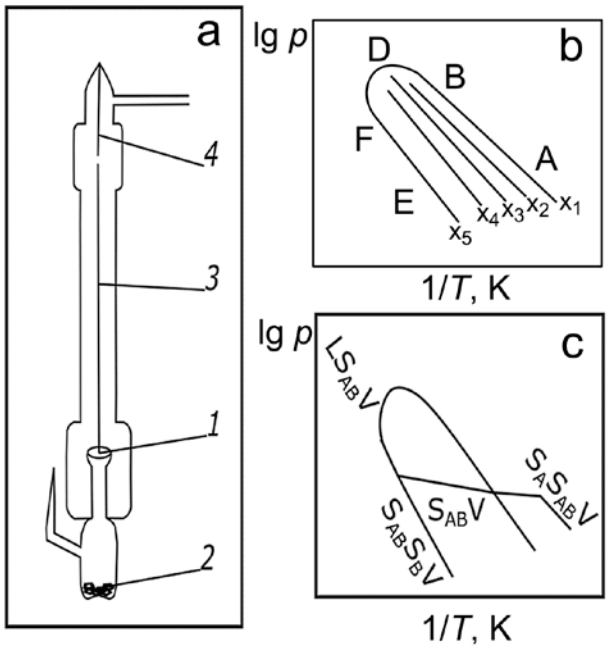

Fig. 7. Possibilities of the tensimetric static method (a) null gauge: plane membrane (*1*), sample (*2*), movable rod (*3*), fixed rod (*4*); (b) *p-T* dependences for the phases with constant compositions x_1-x_5; (c) *p-T* dependence of the AB phase with the homogeneity range

After their classification based on the structural motif with a general chemical formula $(LnR)_2^+(R_2)^{2-}$ (Ln = REM, R = S, Se) and a unique chemical bond [18], dichalcogenides attracted a lot of attention as quasi-two-dimensional layered materials. A double corrugated cationic layer with a NaCl-type structure is combined with a planar anionic layer built of covalently bonded chalcogen dimers in a lattice with a ZrSSi-type structure. With the loss of chalcogen in the anionic layer, vacancies and isolated ions R^{2-} are added to the dimers R_2^{2-}, from which a superstructure forms with a different electron spectrum [19]. However, it proved to be exceptionally difficult to determine the actual scale of nonstoichiometry and the actual structure of REM polychalcogenides. The problem took over 20 years to be solved.

An analysis of the *p-T-x* diagrams of the LnR_2-$LnR_{1.5}$ (Ln = P3M, R = S, Se) systems is based on the dissociation process of the higher polychalcogenide and the reliability of the final data depends heavily on the quality of the initial sample. When finely dispersed chalcogen-absorbing powders of higher polychalcogenides are studied by the gravimetric method, chemical analysis, and powder diffraction, they were identified as phases of variable composition with a wide homogeneity region from LnR_{2+x} to $LnR_{1.70}$ [19–21]. More advanced techniques, namely the STM method and full-field X-ray structure

analysis, were used when crystals were obtained by means of the CVD method and crystallization from flux. Crystals with a size of ~ 1 mm grown under different pressures of chalcogen vapor had different shapes, colors, and macroscopic structural imperfections. Only a few 0.01–0.03 mm crystals could be tested by X-ray structure analysis, whereas in the membranes always the multicomponent mixture of these crystals was placed. The experimental p_S-T-x diagram of the NdS_2-$NdS_{1.50}$ system with four vertical lines of three-phase equilibria S_1S_2V (two solid phases and vapor) divided by horizontal lines of two-phase equilibria S_2V, demonstrates the existence of three intermediate and linear phases $NdS_{1.900}$, $NdS_{1.875}$, and $NdS_{1.857}$ having non-numeric indices (Fig. 8). Their dissociation kinetics takes 5–10 days, and the backwards kinetics takes 30-40 days, which is explained by the formation of any new superstructures in the anionic layer. These compositions normalized to stoichiometric to be phases $Nd_{10}S_{19}$, Nd_8S_{15}, and Nd_7S_{13} with the general formula Nd_nS_{2n-1}, which reflects defectiveness of the anionic layer and its complex inner arrangement.

We should note that lines 2 and 3 do not have any experimental points in the upper parts. This is a direct indication of the impurity nature of phases $NdS_{1.875}$ and $NdS_{1.857}$ located outside or inside the initial disulfide crystals put in the membrane. The fact that the imperfection of most crystals is caused by the mosaic structure and/or fine-scale twinning is supported also by a microscope experiment [22]. Our fractionation of the initial $SmS_{1.9}$ and PrS_2 crystals based on their identical size, shape, and the type of the Raman spectrum was ineffective, because the phase heterogeneity of initial higher crystals was vivid in their p_S-T-x diagrams [23–24], and twin nature of most $SmS_{1.9}$ and PrS_2 crystals was revealed by the structural diagnostics [25–26]. Thus, the realty of phase heterogeneity of the initial crystals of higher polysulfides grown from solution-melts in a wide range of temperatures and pressures of sulfur vapor was confirmed thermodynamically and structurally.

The overview of the thermodynamic, structural, and physical properties of these polysulfide crystals is presented in [27–29]. Taking into account the dependence of the structure formation of

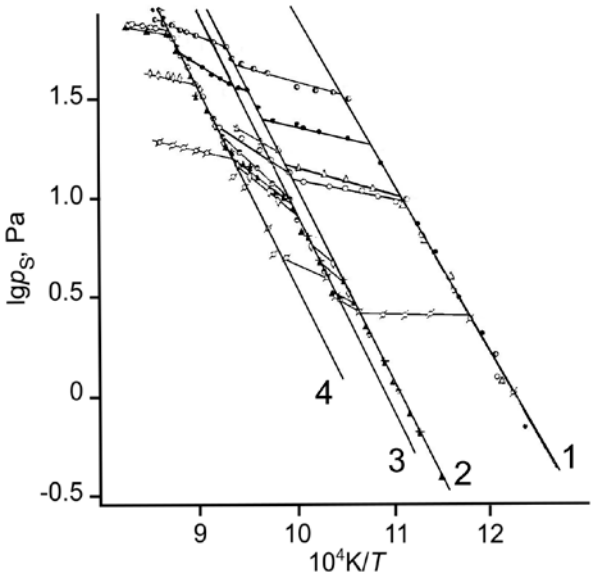

Fig. 8. Experimental Ps-T-x diagram of the NdS_2-$NdS_{1.5}$ system with different m/V (the sample mass / volume of membrane) ratios and monovariant lines *1-4*

intermediate phases on both the thermodynamics (considering also the molecular composition of vapor) and the dissociation kinetics, the STM procedures were elaborated in order to grow larger single-phase and structurally qualitative crystals of higher polysulfides. The adequacy and reliability of the thermodynamic data regarding the composition of the intermediate phase achieved by following operations: expanding the pressure range up to 2 atm and the temperature range up to 1000 °C, decreasing the temperature step to 15 °C, and increasing the exposure time until the composition remains constant at a level of 0.005 at. %. The growing of 4–5 mm crystals from iodide melts and their fractionation based on the shape, density, and spatial chemical homogeneity, ensured the desired quality of the products. The microburette method was used to determine the density of each individual crystal and differential dissolution was applied to control constancy of the atomic Ln/S ratio in time of complete dissolution of the individual crystal. Both methods proved to be effective for the diagnostics of phase and chemical homogeneity of crystals of each from several fractions in which crystals differed in composition and density. With the fraction of homogeneous initial crystals, diagrams of systems $DyS_{1.85}$-$DyS_{1.5}$ [30] and LaS_2-$LaS_{1.5}$ [31-32] reflected actual phase state (Fig. 9) with a smaller number

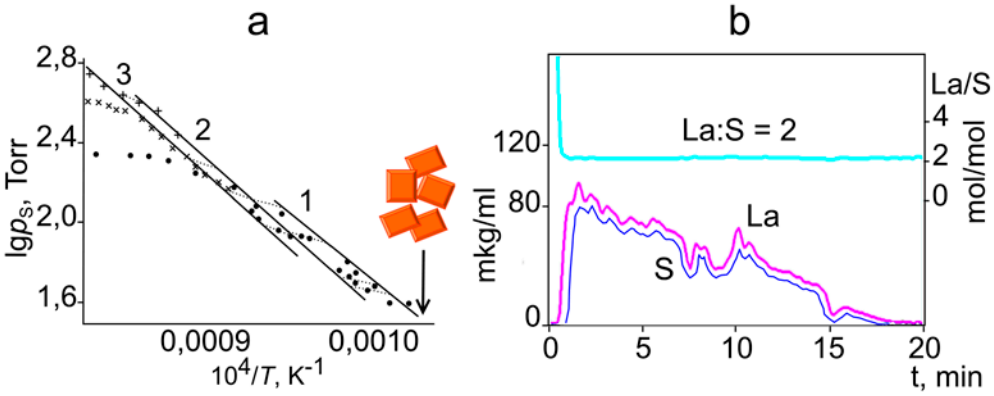

Fig. 9. (a) Experimental *Ps-T-x* diagram of the LaS_2-$LaS_{1.5}$ system for highly homogeneous crystals, monovariant lines (*1–3*) of linear phases LaS_2, $LaS_{1.9}$ and $LaS_{1.76}$; (b) kinetic curves differential dissolution of the homogeneous LaS_2 crystal with stochigram

of coexisting in equilibrium phases than diagrams of non-fractionated crystals. The new type of the diagrams has helped to elucidate the non-equilibrium nature of phases $LaS_{1.96}$, $LaS_{1.87}$, $DyS_{1.81}$, and $DyS_{1.78}$ registered on the previous diagrams. The commonness of occurrence of phase non-equilibrium of polysulfide phases is considered into details in [33].

The homogeneity and microstructural perfection of the $La_{10}S_{19}$ and Dy_8S_{15} crystals ensured the reliability of the quantitative crystal-chemical data relative to the filling factors of all the sulfur positions in the planar anionic layer. For the $La_{10}S_{19}$ phase with 10% of defects, a 10-fold superstructure regarding to structure of the initial ZrSSi subcell was found. For the Dy_8S_{15} with 12.5% of defects, it was already a 24-fold superstructure. Both structures are completely ordered and have geometric proportionality of cationic and anionic layers [31, 34]. The reliability of the chemical and structural data and trustiness of the phase states of the studied systems resulted in classification of Ln polysulfide phases located in the range of 63.7–66.7 at. % of sulfur. The typical phases were LnS_2 (for the La-Nd systems), $LnS_{1.9}$ (for La-Sm), $LnS_{1.85}$ (for Gd-Er), and $LnS_{1.75}$ (for La-Nd). Due to the absence of perfect crystals, phases $LaS_{1.93}$, $DyS_{1.836}$, $HoS_{1.863}$, $DyS_{1.77}$, $NdS_{1.85}$, $SmS_{1.76}$, and $PrS_{1.84}$ with the great structural diversity demonstrate a clear tendency towards disordering of the anionic layer, which could not be realized because of the limited kinetics. Phases $LnS_{2-\delta}$ c $\delta > 0.15$ are characterized by incommensurately modulated structures [26, 35]; the variety of orientations of vacancies, dimers and individual sulfur atoms is considered in [36], where all the studied crystals were twins. In this regard, the authors also believe in correctness of another disordering model, presented as a domain structure of crystals with the domains coherently or incoherently intergrowing with the matrix. Numerous data obtained by the differential dissolution method, which was highly sensitive to the various composition domains located within an individual crystal, confirms the likelihood of the latter model. The pseudomerism masking the actual symmetry of the crystal and the small-scale intergrowing of impurity phases with the matrix are also in good agreement with the results of differential dissolution. Pseudomerism, which is typical for polychalcogenides, is the main source of uncertainty regarding their structural data.

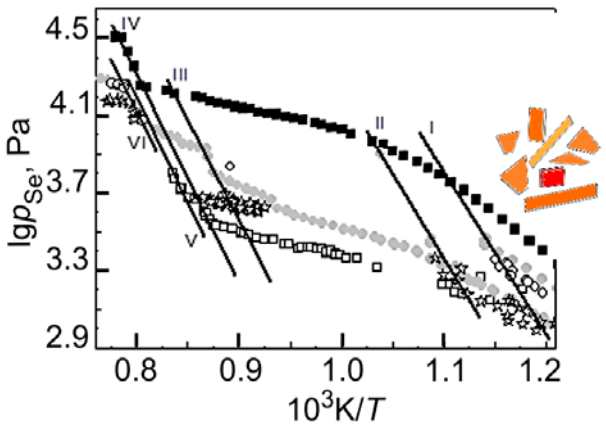

Fig. 10. Experimental p_{Se}-*T*-*x* diagram of the $SmSe_{1.9}$-$SmSe_{1.5}$ system with heterogeneous crystals, monovariant lines *I-YI*, linear intermediate phases $SmSe_{1.875}$, $SmSe_{1.85}$, $SmSe_{1.80}$, $SmSe_{1.75}$, $SmSe_{1.67}$

The thermodynamics of phase transformations in polyselenide diagrams of systems $PrSe_2$-$PrSe_{1.5}$, $GdSe_{1.875}$-$GdSe_{1.5}$, and $SmSe_{1.9}$-$SmSe_{1.5}$ is studied in a different way [37–40]. These experiments were performed with smaller nonfractionated crystals of the initial higher polyselenides and the diagrams of these systems are characterized by a non-reproducible variety of intermediate phases. The diagram of the $SmSe_{1.9}$-$SmSe_{1.5}$ system includes five intermediate phases of closely resembling compositions: $SmSe_{1.90}$, $SmSe_{1.875}$, $SmSe_{1.85}$, $SmSe_{1.80}$, $SmSe_{1.75}$, and $SmSe_{1.67}$ (Fig. 10), most of which, according to the diagram's topology, have a nonequilibrium impurity nature and do not fall into the existing classification of the equilibrium phases of Ln polychalcogenides. The formation of these nonstoichiometric phases complicates the uncontrollable process of the di- and polymerization of selenium in the gas phase during the synthesis, which kinetically hinders the ordering the anionic layer. Nevertheless, such metastable phases continue to attract attention, since the lattice incommensurability of cation-anionic layers is associated with the formation of charge density waves and a good combination of optical, magnetic, and semiconductor properties of the phases [38–39]. In this regard, the conducted physicochemical study significantly contributes to the understanding of the nonstoichiometry of polychalcogenides and the corresponding equilibrium and nonequilibrium structural solid-phase transformations.

4. Stoichiographic differential dissolution method (DD) [4–5]

The effectiveness of the DD method as a key physicochemical tool was especially obvious when analyzing the nonstoichiometry of low-dispersive and amorphous compounds [41–42], as well as thin films with a clear tendency towards spatial inhomogeneity [43–45]. In the DD experiment, the consequent dissolution of phases was performed in a solvent flow with a growing concentration. Based on the analysis of 50–200 portions of the solution, kinetic curves of dissolution of the elements and their stoichiograms are constructed, which after mathematical processing generate data on the number of phases, their composition, and the degree of spatial homogeneity of each individual phase. The effectiveness of the method was demonstrated in [5] and in this review, several special cases are also considered. The color homogeneity of the $[Na_2S]\times Ce_2S_3$ solid solution ensures its popularity as a next generation red pigment. Using the DD method, we determined the phase purity of the powders obtained by solid-phase synthesis at the micro level, as well as the uniformity of the distribution of Na_2S within the grains through fixing invariability the atomic Na/Ce ratio during dissolution of the pigment (Fig. 11). Observed supersaturation of the grain surface with a mobile component Na_2S (that is typical for solid-phase synthesis) resulted in deviation from the standard color value, and

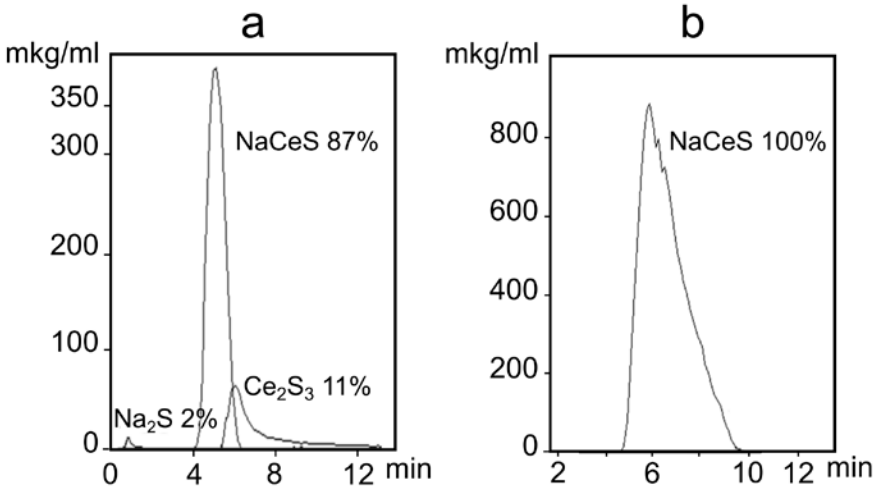

Fig. 11. (a) The phase and chemical composition of the heterogeneous and homogeneous (b) solid solution $Na_2S{\cdot}Ce_2S_3$ according to data of differential dissolution method

only a phase-chemically homogeneous product, giving one peak on the dissolution curves of Na-Ce-S, reflected the quality of pigments with desired color homogeneity [42]. For the $YBa_2Cu_3O_7$ films with a thickness of 0.05-1.0 μm, of vital importance was the data obtained by the DD method regarding the nature and amounts of impurity phases ⩽ 1 wt% and especially their distribution in the film, as well as the determination of sputtering conditions leading to the impurity-free state of the films. The data allowed us to obtain single-crystal specifically oriented films with the best superconducting characteristics of the transition temperature and the current density at that moment [5, 43]. The DD method was used to perform an analysis of the microphase structure of 300 nm films of the ZnS-EuS system. It revealed a very narrow homogeneity region on the level of the $Zn_{0.998}Eu_{0.002}S$ solid solution, which was by an order of magnitude lower than that determined using other trditional methods. This was an important difference, because the appearance of EuS in the form of an impurity phase significantly changed the desired semiconductor properties of the films [44]. MgO thin films are used as effective emitters, and the functional properties are specified to the surface oxygen nonstoichiometry, which is expected to be 10^{-4} at. % at an equilibrium partial pressure of oxygen p_{O_2} = 10^{-9}–10^{-8} Torr. The DD method was successfully in determining of the scale of nonstoichiometry and the conditions favorable for it. It was determined that highly emissive 110 nm MgO films also demonstrated a high chemical activity, due to the formation of a surface layer with oxygen defects. This activity was revealed by dissolving the oxide in hot water. The quantitative data regarding the film dissolution as well as the procedure of creating the required equilibrium partial pressure of oxygen during the film deposition are shown in Fig. 12. We can see that the equilibrium pressure occurs locally in a thin subsurface stationary gas layer due to a heavy dilution of the medium by the release of gaseous products of decomposition of the metal-organic precursor. Heterogeneous equilibrium MgO-O_2 is established according to the reaction $2O_O^X \rightarrow O_{2vapor} + Vö + 2e$, which is alternative to the traditional defect formation process: $Mg_{vapor} \rightarrow Mg_{Mg}^x + Vö + 2e$. The new method of controlling the composition of the oxide phase with oxygen defects does not require highest vacuum or radiation generating surface oxygen vacancies. It is quite simple and is often used in the MOCVD processes [45].

In searching for new materials and structures for emissivity coatings, the greatest attention was paid to pairwise mixed oxides MgO with ZrO_2, RuO_2, or CeO_2, obtained in the form of films by means of MOCVD. However, the nature of the measured emission signal and the emission mechanism were not clear due to the amorphous state of the mixed films. Since a diffraction analysis was here useless, the DD method performed a detailed diagnostics of the phase and chemical state of the films of the

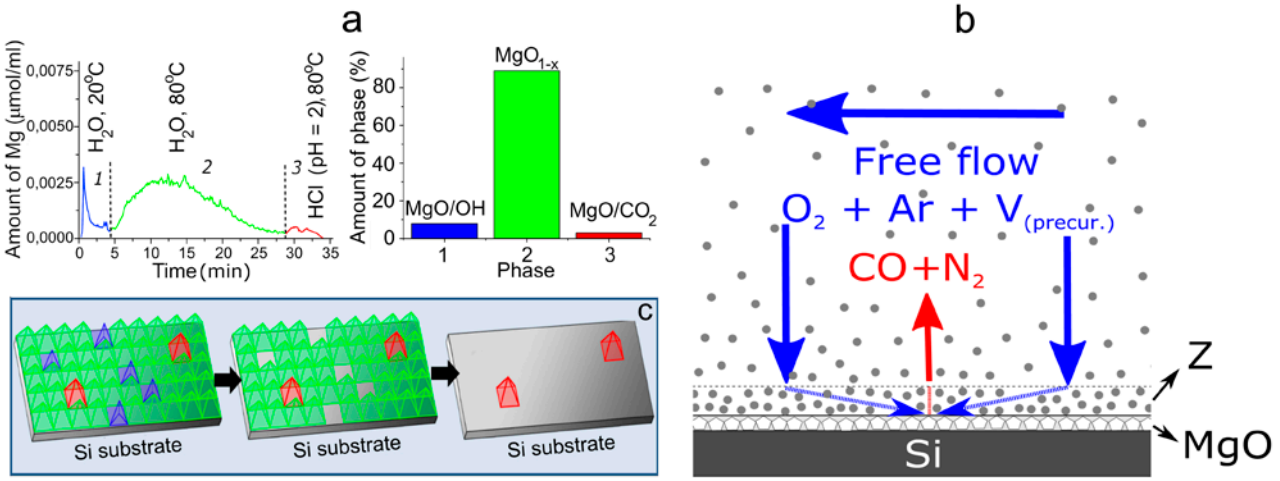

Fig. 12. (a) Kinetic curves of dissolution and phase composition of MgO film; the formation of (b) the gas-near-surface stationary layer Z with p_{O2} = 10^{-9} torr

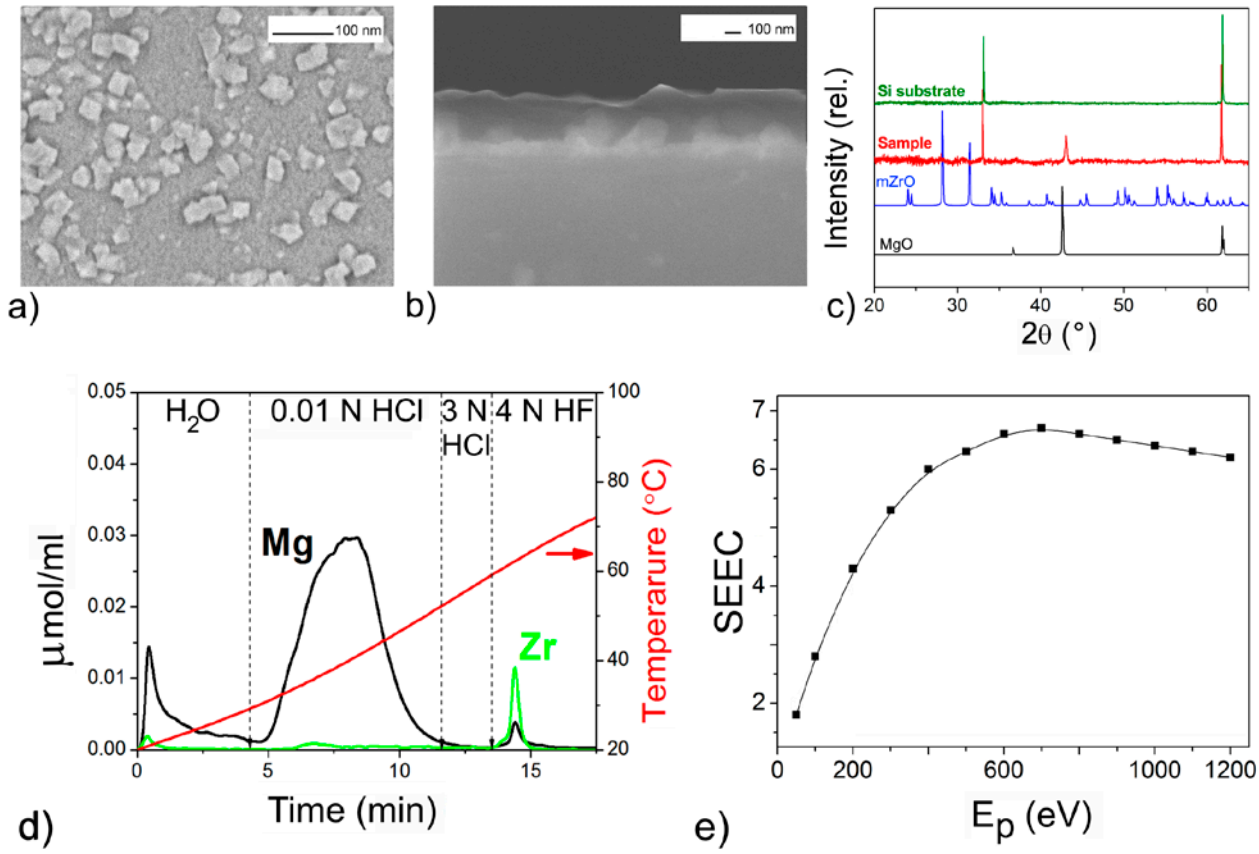

Fig. 13. Characterization of film with the MgO/ZrO_2 = 11/1 composition (a, b) scanning electron microscopy, (c) X-ray diffraction, (d) differential dissolution, (e) coefficient of secondary emission

MgO and ZrO_2 mixture (Fig. 13). It demonstrated that a high chemical activity of both phases, different for MgO and RuO_2, is explained by the oxygen nonstoichiometry of their surfaces resulting from the conditions of film deposition. The active state enabled the oxides to interact and form small fractions of mixed phases based on both oxides Fig. 13. However, the functional properties of the film are determined by its basis, i.e. MgO phase, rather than the mixed impurity phases. In the presented cases, the DD method is the only method that can determine both the phase and chemical state of each from the oxide forms in mixed heterophase films. It facilitates an in-depth understanding of the chemistry and structure of the films and their connection with the functional properties.

5. Conclusions

The review studies the chemistry of promising materials whose compounds melt in the temperature range of 1300–2700 K, but sublimate incongruently, namely LnS, Ln_3S_4, Ln_2S_3, $Yb(Ln)_{14}MnSb_{11}$, $ZrGeO_4$, Zr_3GeO_8, $ZnMo(W)O_4$, $LnS(Se)_2$, and $LnS(Se)_{1.85}$ (Ln – a rare earth element). Due to the specifics of the synthesis of these compounds and their solid-phase and heterophase nature, new physicochemical methods were used to obtain data regarding the nature and dynamics of their transformations. These methods are high-speed high-temperature thermal analysis, static tensimetric membrane technique, and stoichiographic differential dissolution. A combination of the diagnostics methods specific for each compound made it possible to reliably determine the thermodynamic and thermochemical properties of the compounds, as well as the nature of their hightemperature transformations from the initial state to the final product with desired properties. The review demonstrated the importance of accurate *T-x* and *p-T* diagrams of LnS, Ln_2S_3, and $Yb(Ln)_{14}MnSb_{11}$ for the identification of wide and very narrow (up to 10^{-4} at. %) homogeneity regions of the phases.

New data was obtained regarding the lattice mobility of the volatile components of phases $ZrGeO_4$, Zr_3GeO_8, and $ZnMo(W)O_4$ and disordered defective structures of the nonstoichiometric phases of polychalcogenides. The purpose was to review promising methods and approaches to the study of physicochemical systems of various nature and complexity.

Author contributions

I. G. Vasilieva – methodology development, research concept, conducting research, text writing and editing, final conclusions.

Conflict of interests

The author declares that she has no known competing financial interests or personal relationships that could have influenced the work reported in this paper.

References

1. Gibner Ja. I., Vasilyeva I .G. Device for determining the temperatures for phase formations. Patent SU: No. 1806358. Publ. 9.10.1992.

2. Gibner Ja. I., Vasilyeva I. G. Rapid heating in high-temperature thermomicroscopic analysis. *Journal of Thermal Analysis and Calorimetry*. 1998;53: 151–160. https://doi.org/10.1023/a:1010115620439

3. Gibner Ja. I., Vasilyeva I. G. Modified tensimetric set up for the vapor pressure testing*. *Industrial Laboratory*. 1990;56:(7) 45–47. (In Russ.)

4. Malakhov V. V., Vasilyeva I. G. Stoichiography and chemical methods of phase analysis of multielement multiphase compounds and materials. *Russian Chemical Reviews*. 2008;77(4): 370–392. https://doi.org/10.1070/RC2008v077n04ABEH003737

5. Malakhov V. V., Vasilyeva I. G. *Stoichiography: evolution of solid-phase reactions. New principles of research, preparation and characterization of functional materials (book)**. Novosibirsk: Siberian Branch of Russian Academy of Sciences; 2023. 251 c. (In Russ.)

6. Vasilyeva I. G., Nikolaev R. E. Non-stoichiometry and point native defects in non-oxide nonlinear optical large single crystals: advantages and problems. *CrEngComm*. 2019;21: 5890–5897. https://doi.org/10.1039/c9ce01148j

7. Vasilyeva I. G. Nikolaev R. E. High-temperature solid–vapor and liquid–vapor transitions in binary and ternary chalcogenides La_2S_3, MoS_2, Mo_2S_3 and $LiInSe_2$. *Journal of Alloys and Compounds*. 2008;452: 89–93. https://doi.org/10.1016/j.jallcom.2007.01.175

8. Nikolaev R. E. Vasilyeva I. G. Vapor pressure determination for solid and liquid La_2S_3 using boiling points. *Inorganic Materials*. 2008;44(12): 1367–1371. https://doi.org/10.1134/s0020168508120194

9. Gorbunova L. G., Gibner Ja. I., Vasilyeva I. G. The phase diagram of the Nd-S system in the 50-50 at. % S area. *Russian Journal of Inorganic Chemistry*. 1983;29: 222–225.

10. Bien T. N., Hirai S., Vasilyeva I., Nikolaev R., Sekine C., Atsunori K Study of non-stoichiometric GdS_x ($0.68 \leqslant x \leqslant 1.2$) processed by reaction sintering. *Journal of Alloys and Compounds*. 2020;831: 15469. https://doi.org/10.1016/j.jallcom.2020.154691

11. Bien T. N., Hirai S., Vasilyeva I., ... Kawamura Y. Composition and microstructure of holmium monosulfide compacts processed by reaction sintering. *Journal of Alloys and Compounds*. 2021;859: 157872. https://doi.org/10.1016/j.jallcom.2020.157872

12. Abdusalyamova M., Vasilyeva I. The phase equilibrium and intermediate phases in the Eu – Sb system. *Journal of Solid State Chemistry*. 2011;184: 2751–2755. https://doi.org/10.1016/j.jssc.2011.08.018

13. Abdusalyamova M. N., Vasilyeva I. G., Kauzlarich S. The phase equilibrium in Yb-Mn-Sb and Eu-Mn-Sb systems. *SOP Transactions on Physical Chemistry*. 2015;2: 1–9. https://doi.org/10.15764/pche.2015.01001

14. Vasilyeva I. G., Nikolaev R. E., Abdusalyamova M., Kauzlarich S. Thermochemistry study and improved thermal stability of $Yb_{14}MnSb$ alloyed by Ln^{3+} (La-Lu). *Journal of Materials Chemistry C*. 2016;4: 3342–3348. https://doi.org/10.1039/c6tc00178e

15. Vasilyeva I. G., Abdusalyamova M. N., Makhudov F., Eshov B., Kauzlarich S. Thermal air-oxidezed coating on $Yb_{14-x}RE_xMnSb_{11}$ ceramics. The role of rare earth dopants. *Journal of Thermal Analysis and Calorimetry*. 2019;136: 541–549. https://doi.org/10.1007/s10973-018-7659-z

16. Utkin A., Baklanova N., Vasilyeva I. High temperature behavior of zirconium germinates. *Journal of Solid State Chemistry*. 2013;201: 256–261. https://doi.org/10.1016/j.jssc.2013.03.010

17. Vasilyeva I. G., Nikolaev R. E., Nasonov S. G., Kurchev A. V., Shlegel V. N. Peculiarities of the crystallization process and growth of pure nonstoichiometric $ZnMoO_4$ single crystals and those doped with WO_3. *CrystEngComm*. 2019;21: 5890-5897. https://doi.org/10.1039/c9ce01148j

18. Flahauth J., Guittard M., Patrie M. Polysulfides of rare earth metals. *Bulletin de la Société Chimique de France*. 1959;10-12: 1917–1920.

19. Yarembash E. I., Eliseev A. A. *Chalcogenides of rare earth elements**. Moscow: Nauka Publ., 1975, 258 p. (In Russ.)

20. Loginova E. M., Grisik A. A., Ponomarev N. M., Eliseev A. A. The phase *P-T-x* diagram of the La-S system in the La_2S_3-LaS_2 area. Inorganic Materials. 1975;11: 749–751. (In Russ.)

21. Eliseev A. A., Grizik A. A. *Rare earth semiconductors**. Leningrad: Nauka Publ.; 1977. p. 146-177. (In Russ.)

22. Gorbunova L. G., Vasilyeva I. G. Stepped dissociation of the Pr-disulfide*. *Izvestija SO AN SSSR. Serija himicheskih nauk*. 1986;5: 77-81. (In Russ.)

23. Vasilyeva I. G., Belyaeva E. I. Thermodynamic study of the SmS_2-$SmS_{1.5}$ system. *Journal of Solid State Chemistry*. 1999;142: 261–265. https://doi.org/10.1006/jssc.1998.7802

24. Vasilyeva I. G., Belaya S. V. Sulfur nonstoichiometry of PrS_2: a series of new sulfur-deficient phases. *Journal of Solid State Chemistry*. 1999;146: 211–216. https://doi.org/10.1006/jssc.1999.8335

25. Tamazyan R., Arnold H., Molchanov V., Kusmicheva G., Vasilyeva I. The crystal structure and twinning of rare disulfide PrS_2. *Zeitschrift für Kristallographie – Crystalline*

Materials. 2000;215: 272–277. https://doi.org/10.1524/zkri.2000.215.5.272

26. Tamazyan R., Arnold H., Molchanov V., Kusmicheva G., Vasilyeva I. The crystal structure and twinning of $SmS_{1.9}$. *Zeitschrift für Kristallographie – Crystalline Materials*. 2000;215: 346–351. https://doi.org/10.1524/zkri.2000.215.6.346

27. Vasilyeva I. G. Polysulfides. In: *Handbook on the physics and chemistry of rare earths*. K. Gschneider, I. Eyring (eds.). 2001;32: 567–609. https://doi.org/10.1016/s0168-1273(01)32008-1

28. Podberezskaya N., Magarill C., Pervuchina N., Vasilyeva I., Borisov S. Crystallochemical aspects of the structural similarity of rare earth polychalcogenides LnX_{2-x} (x = 0–0.25) *Journal of Structural Chemistry*. 1996; 37: 936–985. https://doi.org/10.1007/bf02439082

29. *Podberezskaya N. V., Pervukhina N. V., Belaya S. V., Vasilieva I. G., Borisov S. V.* Crystal structures of two new holmium polysulfides in the series of rare-earth polychalcogenides. *Journal of Structural Chemistry*. 2001;42(4): 617–627. https://doi.org/10.1023/a:1013198027339

30. Vasilyeva I., Shilkina T., Podberezskaya N., Naumov D. Tensimetric and structural study of dysprosium polysulfides. *Russian Journal of Inorganic Chemistry*. 1999;44(2): 153–156. Available at: https://www.elibrary.ru/item.asp?id=13328511

31. Vasilyeva I., Podberezskaya N., Naumov D., Pervukhina N., Ikorskii V., Borisov S. Growth and structure of lanthanium polysulfide crystals. *Journal of Structural Chemistry*. 2003;44: 154–162. https://doi.org/10.1023/a:1024949418041

32. Vasilyeva I. G., Nikolaev R. E. The La_2S_3-LaS_2 system: thermodynamic and kinetic study. *Journal of Solid State Chemistry*. 2010;183: 1747–1751. https://doi.org/10.1016/j.jssc.2010.05.026

33. Vasilyeva I. G. Phase equilibrium and p_s-T-X-diagrams of the systems Ln_2S_3-LnS_2 (Ln = La, Pr, Nd, Sm-Er). *Russian Journal of Physical Chemistry*. 2006;80: 2068–2073. https://doi.org/10.1134/s003602440611029x

34. Podberezskaya N., Naumov N., Vasilyeva I., Pervuchina N., Magarill C., Borisov S. Structure of dysprosium polysulfide $DyS_{1.83}$(Dy_6S_{11}). according to X-ray diffraction analysis *Journal of Structural Chemistry*. 1998;39: 872-884. https://doi.org/10.1007/bf02903544

35. Graf Ch., Vasilyeva I., Doert Th. Six new rare earth polysulfide compounds with ZrSSi superstructure: $LnS_{1.85(2)}$ (Ln = Y, Gd – Er). Technische Universität Dresden: *Gemainsame Jahrestagung* der Deutschen Gesellschaft fur Kristallographie und der Deutschen fur Kristallzuchtung, Universitat Bremen, 5–9 Marz, 2007.

36. Doert Th., Graf Ch., Vasilyeva I., Schnelle W. Structural frustration and occupational disorder: the rare earth metal polysulfides $Tb_8S_{14.8}$, $Dy_8S_{14.8}$, $Ho_8S_{14.8}$, $Y_8S_{14.8}$. *Inorganic Chemistry*. 2012;51: 282–289. https://doi.org/10.1021/ic201639f

37. Zelenina L., Chusova T., Vasilyeva I. Thermodynamic investigation of the phase formation processes in the systems $LnSe_2$–$LnSe_{1.5}$ (Ln = La, Ce, Pr, Nd). *The Journal of Chemical Thermodynamics*. 2013;57: 101–107. https://doi.org/10.1016/j.jct.2012.08.005

38. Doert Th., Graf Ch., Schmidt P., Vasilyeva I., Simon P., Carrillo-Cabrera W. The $PrSe_2$-$PrSe_{1.5}$ system: studies of the phase relationships and the modulated crystal structure of $PrSe_{1.85}$. *Journal of Solid State Chemistry*. 2007;180: 496-509. https://doi.org/10.1016/j.jssc.2006.10.030

39. Chusova T. P., Zelenina L. N., Vasilyeva I. G., Graf Ch., Doert Th. Thermodynamic study of the system $PrSe_2$-$PrSe_{1.5}$ and $GdSe_{1.875}$-$GdSe_{1.50}$. *Journal of Alloys and Compounds*. 2008;452: 94–98. https://doi.org/10.1016/j.jallcom.2006.12.162

40. Zelenina L. N., Chusova T. P., Vasilyeva I. G. Thermodynamic properties of Sm-and Gd-polyselenides. *The Journal of Chemical Thermodynamics*. 2015;90: 122–128. https://doi.org/10.1016/j.jct.2015.06.031

41. Vasilyeva I. G., Logvinenko V. A. Contribution of chemical methods in the study of nanostructures of ultrafine and amorphous materials. *Solid State Phenomena*. 2016;257: 237–240. https://doi.org/10.4028/www.scientific.net/ssp.257.237

42. Vasilyeva I., Ayupov B., Vlasov A., Malakhov V., Macaudiere P., Maestro P. Color and chemical heterogeneities of γ-[Na]-Ce_2S_3 solid solutions. *Journal of Alloys and Compounds*. 1998;268: 72–77. https://doi.org/10.1016/s0925-8388(97)00580-x

43. Vasilyeva I. G., Malakhov V. V., Vlasov A. A., Predtechensky M. R. New method of microphase and chemical analysis as applied to the YBaCuO thin films. *Thin Films*. 1997;292: 85–90. https://doi.org/10.1016/s0040-6090(96)08945-6

44. Vasilyeva I., Ivanova E., Vlasov A., Malakhov V. Phase composition of mixed ZnS-EuS thin films grown by metal organic chemical vapor deposition. *Materials Research Bulletin*. 2003;38: 409–415. https://doi.org/10.1016/s0025-5408(02)01070-x

45. Vasilyeva I. G., Vikulova E. S., Pochtar A. A., Morozova N. B., Igumenov I. K. Invisible surface oxygen vacancies in a thin MgO film: impacts on the chemical activity and secondary electron emission. *Inorganic Chemistry*. 2020;59: 17999–18009. https://doi.org/10.1021/acs.inorgchem.0c02351

46. Vasilyeva I. G., Vikulova E.S., Pochtar A. A., Morozova N. B. Mixed films based on MgO for secondary electron emission application general trends and MOCVD Prospects. *Coating*. 2021;11: 176–194. https://doi.org/10.3390/coatings11020176

** Translated by author of the article*

Information about the author

Inga G. Vasilyeva, Dr. Sci. (Chem.), Leading Research Fellow of Nikolaev Institute of Inorganic Chemistry Siberian Branch of RAS (NIIC SB RAS) (Novosibirsk, Russian Federation).

https://orcid.org/0000-0003-4045-9820

kamars@niic.nsc.ru

Received 21.06.2024; approved after reviewing 01.07.2024; accepted for publication 16.09.2024; published online 16.09.2024;

Translated by Yulia Dymant